TITLE: CHATTER STABILITY ANALYSIS APPROACH FOR STABILITY ANALYSIS OF ROTATING

MACHINERY VIBRATIONS

AUTHORS: Erol TÜRKES

PAGES: 1-17

ORIGINAL PDF URL: https://dergipark.org.tr/tr/download/article-file/325724

CHATTER STABILITY ANALYSIS APPROACH FOR STABILITY ANALYSIS OF ROTATING MACHINERY VIBRATIONS

Erol Türkeş[*1]

Kırklareli University, Department of Mechanical Engineering, Kayalı Campus. Kırklareli/TÜRKİYE

erol.turkes@klu.edu.tr

Abstract

Vibration caused by mass imbalance is an important factor limiting the performance and fatigue life of the rotating system. Therefore, a balancing procedure is necessary for rotating systems. Spindle is the main mechanical component in machining centers. Its performance has a direct impact on the machining productivity and surface quality of the workpiece. In this paper, regenerative chatter analysis approach is used for vibrations of rigid rotors with a massless elastic shaft. This approach is firstly applied in literature by this study. In this study, Stability Lobe Diagram (SLD) is plotted the boundary between stable and unstable rotations as a function of spindle speed and imbalance mass. SLD process can be easily applied between spindle length, balancing mass amount, location of balancing mass on rotor etc. variable parameters and spindle speeds for stable rotating system.

Key words: Rotating machinery, Vibration, Stability analysis

DÖNER MAKİNA TİTREŞİMLERİNİN STABİLİTE ANALİZİ İÇİN TIRLAMA STABİLİTE ANALİZİ YAKLAŞIMI

Özet

Kütle dengesizliğinden kaynaklanan titreşim, döner sistemlerin performansını ve yorulma ömrünü sınırlayan önemli bir etkendir. Bu sebeple döner sistemler için bir dengeleme işlemi gereklidir. Mil, işleme merkezlerinin en önemli bileşenidir. Onun performansının işleme verimliliği ve işlenen parçanın yüzey kalitesi üzerinde direkt etkisi vardır. Bu çalışmada, rejeneratif tırlama analizi yaklaşımı, kütlesiz elastik şaftlı rijit rotorların titreşimlerinde kullanılmıştır. Bu yaklaşım literatürde ilk olarak bu çalışmada uygulanmıştır. Bu çalışmada Stabilite Lob Diyagramı (SDD), mil hızı ve dengesizlik kütlesinin bir fonksiyonu olarak kararlı ve karasız dönüşler arasındaki sınırda çizilmiştir. SLD, mil uzunluğu, dengeleyici kütle miktarı, dengeleyici kütlenin konumu vb. değişken parametreler ile stabil döner sistemlerin mil hızları arasında kolaylıkla uygulanabilir.

Anahtar Kelimeler: Döner Makineler, Titreşim, Stabilite Analizi

*[*1] Erol Türkeş, erol.turkes@klu.edu.tr*

1. INTRODUCTION

Rotating machine elements are commonly used in mechanical systems. For example, machine tools, aircraft gas turbine engines etc. have rotating equipment. Vibration due to mass imbalance is a general issue in rotating machine elements. Imbalance occurs if the rotating axis of inertia of the rotating machine element (rotor) is not coincident with geometric axis of rotating machine element. As known, higher spindle speeds generate much greater centrifugal imbalance forces. Hence, the tendency of the rotating machine element towards high power requirements leads to higher operating speeds. Generally, chatter vibrations are one of the most critical limiting factors considered in machine tool design. The centrifugal force on rotating cutting system of machine tool becomes periodically variable, reaching considerable amplitudes and machine tool system becomes shutdown. Therefore, vibration suppression of rotating machine element is difficult and important engineering problem. Vibration control is necessary in achieving longer bearing life, spindle life, and tool life in high-speed machining. Also, vibration control is very important for improving machining surface finish and reducing the number of unexpected shutdowns. Significant cost savings for high-speed turbines, compressors etc. and power generation stations can be achieved using a variety of vibration control analysis methods [1, 2]. Many techniques have been presented to reduce within acceptable limits this vibration on machines: off-line balancing methods [3], on-line active balancing methods using mass redistribution devices [4-7], and on-line active balancing methods using magnetic bearings [8-11]. These on-line methods can be applied during rotor operation if the rotation speed is constant.

The manufacture process in many factories is extremely automated and requires which the turning, milling, drilling and grinding operations run for predictable time periods to maintaining production throughput. This means that with existing cutting tools and equipment, machine tools must operate at a range of operating speeds up to 12,000 rpm, with an unplanned number of holds. Today's modern machine tools can operate from 16,000 rpm up to a maximum of 80,000 rpm. There is a need to apply High Speed Machining (HSM) technology to new areas to increase productivity, reduce costs and delivery time, and increase processing sensitivity of complex features. Cutting performance in HSM is driven primarily by tool holder, tool and spindle dynamics. Generally, vibration analysis can be easily discriminated from oscillation effects of machine tools due to the much stricter and lower frequency dynamics of the structure of machine tools. Cutting tool and work spindle of machine tool interaction critical and difficult to intuitively predict. Machine tools consist of a machining process, a machining process model, a structural model and a feedback loop. The cutting force on the cutting tool depends on the feed rate, cutting depth and cutting speed. This dynamic shear forces cause a relative displacement between the tool and the

workpiece by stimulating the structural model of the tool and/or workpiece. These displacements then modulate the cutting feed and/or depth by means of the displacement feedback and possibly cause excited instability. To solve the stability problem, the system characteristic equation can be derived and solved to obtain the stability limit with respect to the depth of cut. Problem of rotating cutting tool of machine tool can be analyzed in one of two methods. The stability analysis can be carried out at stationary inertia coordinates; the directional coefficients of the force components in these coordinates change periodically with time. Or, this stability analysis can be done in the rotating coordinate space of the cutting tool, in which case the directional force coefficients are not time dependent. However, in the latter method, the two orthogonal coordinates of the cutting tool are dynamically combined as a function of spindle speed. For rotary tool machining, such as milling, drilling and cylinder drilling, the tool rotation causes the machining force on each tooth to rotate repeatedly with respect to the inertia coordinate frame. This is different than stationary tool machining, such as turning or boring in which the force directions are fixed relative to the inertial frame. Stability analysis for rotating tools is extensively investigated in the milling and grinding process, but the process is interrupted and therefore changes over time, leading to analysis methods that are analytically approximate or use time domain simulations [12]. In this study, a chatter stability analysis approach for stability analysis of a rigid rotor's vibrations is presented. This approach was firstly applied for rigid rotors as rotating shaft. Stability Lobe Diagram (SLD) is plotted the boundary between stable and unstable rotations as a function of spindle speed of machine tools and imbalance mass. Therefore, firstly, modal analysis is performed for spindle-rotor system in perpendicular to each other direction. Model analysis of the cutting system is performed by impact force hammer set and CutPro 8 software. Hence, equivalent mass, damping ratio, stiffness and natural frequency of spindle-rotor system are determined. Acting forces on the rotor are determined by a force dynamometer.

2. MODELING OF DYNAMIC ROTOR SYSTEM

The planar rotor model (PRM) is the simplest model for mathematical modeling. Because, only the motion of dynamic rotor system in the plane (x-y), that is perpendicular to the rotating elastic spindle (shaft), is take into accounted. Even though the PRM is pretty simple rotor model, as critical speed, damping effect, it can be used to investigate the principal phenomenon of rotating disc dynamics as well. The rotor in the PRM is modeled as a rigid disc supported by a massless elastic spindle mounted on stationary solid bearings. Also, it is suitable to a solid spindle supported by elastic bearings. A significant development over the simple PRM is which the movement of the rotor is shown by solid form movement instead of

particle movement. Although PRM is a single solid rotating disc (rotor) model, it can represent the basic some event in the movement of the rotor, including the forward and backward whirling under imbalance force, the gyroscopic effect, critical speeds, and so on. In fact, the natural frequency of the system is a function of the number of cycles (spindle speed) that can be estimated by this PRM. The geometric and force setup of the planar rotor model is shown in Figure 1. In this model, the vibration caused by the imbalance is defined by the particle motion of the discrete geometric center. Here, P is the discrete geometric center and G is the discrete mass center.
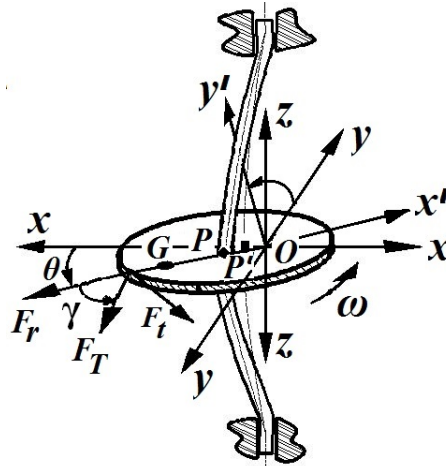

Figure 1. Geometric and Force Setup of the Rigid Rotor Model

Where, θ is the rotating angle of the rotor, x, y, z are rotor coordinate frame through the geometric center of the shaft and/or of the disc (O), x', y' are coordinate transformation with θ. P is the geometric center of the disk, P' is the displacement of the P due to vibration and G is the mass center of the disk. F_r, F_t and F_T are radial, tangential and centrifugal total forces respectively. The equations of motion of the rotating system with a constant spindle speed (ω_z), can be derived in the rotational coordinates;

$$m_x\,\ddot{x}(t) + c_x\,\dot{x}(t) + k_x\,x(t) = -F_{Tx}(t)$$
$$m_y\,\ddot{y}(t) + c_y\,\dot{y}(t) + k_y\,y(t) = -F_{T_y}(t) \tag{1}$$

where $m_{x,y}$, $c_{x,y}$, and $k_{x,y}$ are the mass, the viscous damping coefficient, and the shaft-stiffness coefficient on the x and y directions, respectively. Total force $(F_T(t))$ is can be expressed as;

$$F_T(t) = \sqrt{F_r(t)^2 + F_t(t)^2} \tag{2}$$

where radial $\left(F_r(t)\right)$ and tangential $\left(F_t(t)\right)$ forces are can be expressed as;

$$F_r(t) = m_b \, \vec{a}_x^n(t) = m_b \, h(t) \, \vec{\omega}_z^2(t)$$

$$F_t(t) = m_b \, \vec{a}_x^t(t) = m_b \, h(t) \, \vec{\alpha}_z(t) \tag{3}$$

Where m_b is imbalance mass of the rotating disc. For a constant rotating speed $\left(\dot{\theta}(t) = \vec{\omega}_z(t) = \vec{\omega}_z = cons.\right)$, $\ddot{\theta} = \alpha$ is zero. If angular acceleration is not zero $\left(\alpha \neq 0\right)$, the equations of motion of the system are expressed as;

$$m_x \, \ddot{x}(t) + c_x \, \dot{x}(t) + k_x \, x(t) = -F_{Tx}(t) = -F_T(t) \cos \theta(t) \cos \gamma(t)$$

$$m_y \, \ddot{y}(t) + c_y \, \dot{y}(t) + k_y \, y(t) = -F_{T_y}(t) = -F_T(t) \sin \theta(t) \sin \gamma(t) \tag{4}$$

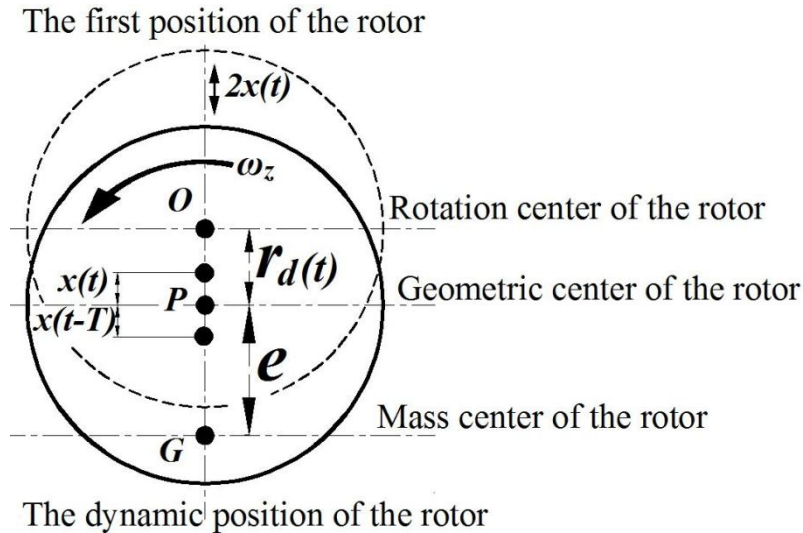Where γ is angle between $F_T(t)$ and $F_r(t)$ as shown in Fig.3.

Figure 2. Dynamic position system of the Rigid Rotor Model

Equations (2) and (3) are substituted into Equation (4);

$$m_x \, \ddot{x}(t) + c_x \, \dot{x}(t) + k_x \, x(t) = -m_d \, h(t) \sqrt{\omega_z^4(t) + \alpha_z^2(t)} \, \cos \theta(t) \cos \gamma(t)$$

$$m_y \ \ddot{y}(t) + c_y \ \dot{y}(t) + k_y \ y(t) = -m_d \ h(t) \sqrt{\omega_z^4(t) + \alpha_z^2(t)} \ \sin\theta(t)\sin\gamma(\mathrm{t}) \tag{5}$$

Where $Q(t) = \sqrt{\omega_z^4(t) + \alpha_z^2(t)}$. If angular acceleration is zero $(\alpha \neq 0)$, the equations of $Q(t)$ is

$Q(t) = \sqrt{\omega_z^4(t)}$ and $\gamma = 0 \implies F_T(t) = F_r(t)$. Combining this term with Eq. (5) gives;

$$m_x \ \ddot{x}(t) + c_x \ \dot{x}(t) + k_x \ x(t) = -m_d \ h(t) \ Q(t)\cos\beta(t)$$

$$m_y \ \ddot{y}(t) + c_y \ \dot{y}(t) + k_y \ y(t) = -m_d \ h(t) Q(t) \ \sin\beta(t) \tag{6}$$

where $h(t) = \overrightarrow{OG}(t)$ is dynamic displacement of through the geometric center of the disk as shown in Fig.1 and Fig.2 and, β is angle between $F_T(t) = F_r(t)$ and mode x direction as shown in Fig.3. Hence, dynamic displacement $(h(t))$ is can be written as;

$$h(t) = O\vec{G}(t) = e + r_d(t) = e + r_d - x(t) + x(t - \tau) \tag{7}$$

where $e = |PG|$ is eccentricity between P and G and constant, $x(t) = \overrightarrow{PP'}(t)$ is the present

displacement of the geometric center of the disk from the static position (O), $x(t - \tau) = \overrightarrow{OP'}(t)$ is the displacement of the geometric center of the disk on the previous rotation with the amount of θ of the disk. Also, $r_d(t) = r_d - x(t) + x(t - \tau)$ is displacement between rotation center of the rotor (during static of the rotor) (O) and geometric center of the rotor (during dynamic of the rotor) (P) of the rotor system. The values of the $r_d(t)$ can be obtained from the case of a centrifugal force equal to the shaft deflection force (Hook's law);

$$F_{shaft}(t) = F_{centr.}(t) \implies k \ r_d(t) = m \ \omega_z^2 \left[r_d(t) + e \right]$$

$$\frac{k}{m} r_d(t) = \omega_z^2 \left[r_d(t) + e \right] \rightarrow \omega_n^2 = \frac{k}{m}$$

$$\omega_n^2 r_d(t) = \frac{k}{m} r_d(t) = \omega_z^2 \left[r_d(t) + e \right] \rightarrow r = \frac{\omega_z}{\omega_n}$$

$$r^2 = \frac{r_d(t)}{\left[r_d(t) + e \right]} \tag{8}$$

By resonance condition of the rotating rotor system;

$$\omega_z^2 = \frac{\omega_n^2 \, r_d(t)(1-r)}{e} \qquad \rightarrow \qquad r_d(t) = e \, \frac{r^2}{(1-r^2)} \tag{9}$$

Hence, plotting of the stability lobes can be achieved by scanning the chatter frequencies $\left(\omega_c = \omega_z\right)$

around the natural frequency $\left(\omega_n\right)$ of the structure for the $r = \dfrac{\omega_z}{\omega_n} = \dfrac{\omega_c}{\omega_n}$.
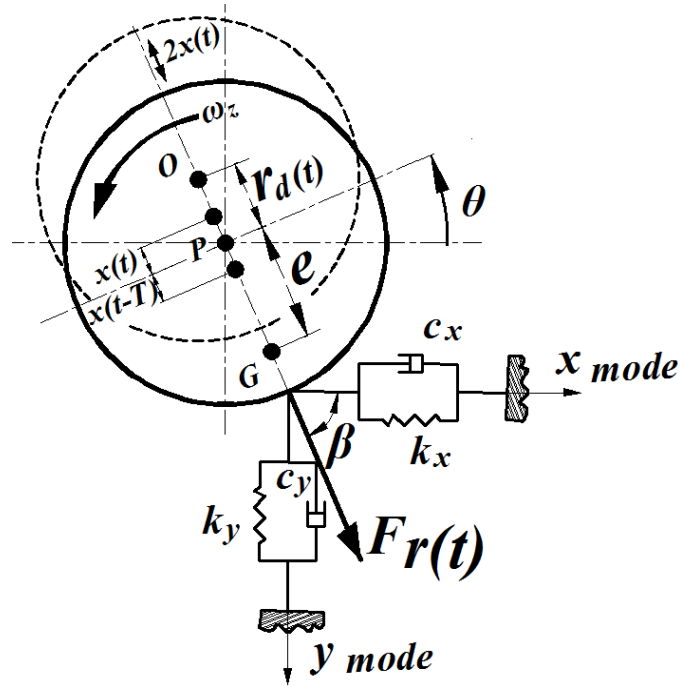

Figure 3. Vibration modes and Radial force $\left(F_r(t)\right)$ of the dynamic rigid rotor system.

However, for this article $\ddot{\theta} = \alpha$ is zero. Hence, Eq. (6) can be written as;

$$m_x \, \ddot{x}(t) + c_x \, \dot{x}(t) + k_x \, x(t) = -m_d \, h(t) \, \omega_z^2(t) \cos \, \beta(t)$$

$$m_y \, \ddot{y}(t) + c_y \, \dot{y}(t) + k_y \, y(t) = -m_d \, h(t) \, \omega_z^2(t) \sin \, \beta(t) \tag{10}$$

Defining the following terms;

$$K_x(t) = C \, \cos \, \beta(t); \; K_y(t) = C \, \sin \, \beta(t) \qquad \rightarrow \qquad C = \omega_z^2(t) = cons.$$

The equations of motion can be written as;

$$m_x \, \ddot{x}(t) + c_x \, \dot{x}(t) + k_x \, x(t) = -K_x(t) \, m_d \, h(t)$$

$$m_y \, \ddot{y}(t) + c_y \, \dot{y}(t) + k_y \, y(t) = -K_x(t) \, m_d \, h(t) \tag{11}$$

By defined the following terms from Eq.(7); $\quad e + x(t-\tau) = x(t-\tau); \quad r_d - x(t) = x(t).$

Combining these terms with Eq. (11) gives;

$$m_x\,\ddot{x}(t) + c_x\,\dot{x}(t) + k_x\,x(t) = -K_x(t)\,m_d\left[x(t) - x(t-\tau)\right]$$

$$m_y\,\ddot{y}(t) + c_y\,\dot{y}(t) + k_y\,y(t) = -K_x(t)\,m_d\left[x(t) - x(t-\tau)\right] \tag{12}$$

The equations of motions are converted to a form in terms of arc length, (u), instead of time (t) defined as follows:

$$u = V\,t \qquad \Rightarrow \qquad u_t = \frac{du}{dt} = V$$

where V is the mean linear speed of the disk given by:

$$V = \frac{\pi\,d\,n}{60}$$ and, where d is the disk diameter $[m]$, n is spindle speed $[rpm]$. For convenience, the dimensionless equations of motion for this spindle are:

$$m_x\left(\frac{du}{dt}\right)^2 x'' + c_x\left(\frac{du}{dt}\right)x' + k_x\,x = -K_x(t)\,m_d\left[x(u) - x(u - d\pi)\right]$$

$$m_y\left(\frac{du}{dt}\right)^2 y'' + c_y\left(\frac{du}{dt}\right)y' + k_y\,y = -K_y(t)\,m_d\left[x(u) - x(u - d\pi)\right] \tag{13}$$

Furthermore, the equations are then simplified somewhat by dividing the x-direction equation through by $m_x\left(\frac{du}{dt}\right)^2 = m_x\,V^2$ and the y-direction equation by $m_y\left(\frac{du}{dt}\right)^2 = m_y\,V^2$ and defining the following terms;

$$\tilde{c}_x = \frac{c_x}{m_x\,V}\ , \qquad \tilde{k}_x = \frac{k_x}{m_x\,V^2}\ , \qquad \tilde{F}_x = \frac{-K_x\,m_d}{m_x\,V^2}$$

$$\tilde{c}_y = \frac{c_y}{m_y\,V}\ , \qquad \tilde{k}_y = \frac{k_y}{m_y\,V^2}\ , \qquad \tilde{F}_y = \frac{-K_y\,m_d}{m_y\,V^2}$$

By simplifications the equations of motion are gives;

$$x'' + \tilde{c}_x\,x' + \tilde{k}_x\,x = \tilde{F}_x\left(x(u) - x(u - d\pi)\right)$$

$$y'' + \tilde{c}_y\, y' + \tilde{k}_y\, y = \tilde{F}_y \left(x(u) - x(u - d\pi) \right) \tag{14}$$

To obtain of the characteristic equation of system, the equations of motion can be written in matrix form as [13];

$$\begin{bmatrix} 1 & 0 \\ 0 & 1 \end{bmatrix} \begin{Bmatrix} x'' \\ y'' \end{Bmatrix} + \begin{bmatrix} \tilde{c}_x & 0 \\ 0 & \tilde{c}_y \end{bmatrix} \begin{Bmatrix} x' \\ y' \end{Bmatrix} + \begin{bmatrix} \tilde{k}_x - \tilde{F}_x & 0 \\ -\tilde{F}_y & \tilde{k}_y \end{bmatrix} \begin{Bmatrix} x \\ y \end{Bmatrix} + \begin{bmatrix} \tilde{F}_x & 0 \\ \tilde{F}_y & 0 \end{bmatrix} \begin{Bmatrix} x(u - d\pi) \\ y(u - d\pi) \end{Bmatrix} = \begin{Bmatrix} 0 \\ 0 \end{Bmatrix} \tag{15}$$

Taking the Laplace Transform and determinant to find the characteristic equation of system yields;

$$E(s) = s^4 + \left(\tilde{c}_x + \tilde{c}_y \right) s^3 + \left(\tilde{k}_y + \tilde{c}_x\, \tilde{c}_y + (\tilde{k}_x - \tilde{F}_x) \right) s^2 + \left(\tilde{c}_x\, \tilde{k}_y + \tilde{c}_y\, (\tilde{k}_x - \tilde{F}_x) \right) s +$$
$$\tilde{k}_y \left(\tilde{k}_x - \tilde{F}_x \right) + \left(s^2 + \tilde{c}_y\, s + \tilde{k}_y \right) \tilde{F}_x\, e^{-sd\pi} \tag{16}$$

where;

$$a_4 = 1/\tilde{F}_x\,, \qquad a_3 = \left(\tilde{c}_x + \tilde{c}_y \right)\!/\tilde{F}_x\,, \qquad a_2 = \left(\tilde{k}_y + \tilde{c}_x\, \tilde{c}_y + (\tilde{k}_x + \tilde{F}_x) \right)\!/\tilde{F}_x$$
$$a_1 = \left(\tilde{c}_x\, \tilde{k}_y + \tilde{c}_y\, (\tilde{k}_x + \tilde{F}_x) \right)\!/\tilde{F}_x\,, \qquad a_0 = \tilde{k}_y \left(\tilde{k}_x + \tilde{F}_x \right)\!/\tilde{F}_x$$

Combining these terms with (16) gives:

$$E(s)/\tilde{F}_x = a_4\, s^4 + a_3\, s^3 + a_2\, s^2 + a_1\, s + a_0 + \left(s^2 + \tilde{c}_y\, s + \tilde{k}_y \right) e^{-sd\pi} \tag{17}$$

Setting $E(s)$ equal to 0, this becomes:

$$e^{sd\pi} = \frac{-\left(s^2 + \tilde{c}_y\, s + \tilde{k}_y \right)}{a_4\, s^4 + a_3\, s^3 + a_2\, s^2 + a_1\, s + a_0} \tag{18}$$

Equation (18) is then separated into two parts:

$$U_1 = e^{s\pi d}\,, \quad U_2 = -\frac{s^2 + \tilde{c}_y s + \tilde{k}_y}{a_4 s^4 + a_3 s^3 + a_2 s^2 + a_1 s + a_0} \tag{19}$$

Letting $s = j\omega$ the roots of $E(s)$ will occur when $\left| U_2(j\omega) \right| = 1$ therefore:

$$1 = \frac{\left|\left(\tilde{k}_y - \omega^2\right) + j\tilde{c}_y\omega\right|}{\left|\left(a_4\omega^4 - a_2\omega^2 + a_0\right) + j\left(a_1\omega - a_3\omega^3\right)\right|} \tag{20}$$

Eq.(20) is squared resulting in the following:

$$\left(\tilde{k}_y - \omega^2\right)^2 + \tilde{c}_y^{\;2}\omega^2 = \left(a_4\omega^4 - a_2\omega^2 + a_0\right)^2 + \left(a_1\omega - a_3\omega^3\right)^2 \tag{21}$$

Expanding this and collecting terms yields:

$$a_4^2\omega^8 + \left(-2a_4a_2 + a_3^2\right)\omega^6 + \left(2a_4a_0 + a_2^2 - 2a_3a_1 - 1\right)\omega^4 +$$
$$\left(-2a_2a_0 + a_1^2 + 2\tilde{k}_y - \tilde{c}_y^{\;2}\right)\omega^2 + a_0^2 - \tilde{k}_y^{\;2} = 0 \tag{22}$$

The roots of this equation can now be found. Since (20) was squared to produce (22), the number of found roots will be twice the number actually found in the system. As a result, only the positive real roots of the equation need to be examined. Each positive real root ω_i is substituted back into (19) to find $U_2(j\omega_i)$. The angle of the resulting number is calculated as follows:

$$\alpha_i = \tan^{-1}\frac{\text{Im}\left(U_2(j\omega_i)\right)}{\text{Re}\left(U_2(j\omega_i)\right)} \tag{23}$$

The angle is then used to generate the values of the delay values, τ, where;

$$\tau_{ik} = \left(\alpha_i + 2k\pi\right)/\omega_i \qquad\qquad \text{k=0, 1, 2, ...} \tag{24}$$

One of these sequences is produced for each root. Sequences of all these roots are brought together and sorted in ascending order. This sequence represents intervals on the time delay axis. These delay values are computed at each positive real root and gives a large set for $(k = 1, 2, 3, ...)$ The total set of delays are then brought together in an increasing order to form intervals of the τ axis.

3. STABLITY ANALYSIS OF ROTOR SYSTEM

Vibration due to mass imbalance is one of the important factors limiting the performance of a rotating system and the fatigue life. There are two important control methods for suppressing vibration caused by imbalance. These are active and passive control methods. Both methods are used to balance the rotating

system. Active vibration control is more effective and more flexible than passive vibration control. It is therefore more useful. There are also two types of active vibration control techniques. These are direct active vibration control techniques and active balancing techniques. Off-line balancing methods in active balancing techniques [3] are widely used in practice. Even so these techniques are usually time-consuming and cannot be used if the distribution of imbalance changes during operation. In some studies as in [4-7] was tried to use some kind of mass redistribution device to actively balance the rotating systems during operation. This method can be used to determine the vibration caused by the imbalance or the force transmitted to the base, lateral force actuators such as magnetic bearings [8-11]. All of the above-mentioned investigations focus on the constant rotation speed condition. This is called the "steady state". Due to the assumption of constant speed of rotation, the rotor coefficient method is used to model the dynamic rotor system. All rotor dynamics equations are constructed with constant influence coefficients. Estimation of the imbalance, which is very important in the balancing and active vibration control schemes, is carried out by estimating the effect coefficients. An alternative method to estimate the rotating system imbalance is provided by Reinig and Desrochers [14] and Zhu et al. [15]. States of the rotor dynamic system are increased to include imbalance forces. Then, an observer is used to estimate the determined increased states in their methods. Their methods are also related to the constant spindle speed case. For this reason, the magnified system is a time-invariant linear system. Luenberger observer (Luenberger [16]) can be used to estimate the imbalance forces. In addition to the constant spindle speed (rpm), the imbalance vibration control must be completed for a time-varying transient time to save time and improve performance in some other situations. For example, a machining tool must be subjected to a cutting process in which the spindle enters a steady state during high-speed machining. To reduce the effect of the cutting tool vibration during the cutting cycle, the machine tool's vibration control must be active during acceleration time. Although several researchers as in (Knospe et al. [17]) have indicated how to conduct imbalance vibration control during the startup through the critical speed, their basic method is to interpolate the influence coefficients between different speeds. This is a quasi-steady strategy. Very little research has been done with rapid acceleration and low damping rate for balancing and active control of the rotor system. Zhou and Shi [18] obtained an analytical expression of the vibration that induced the imbalance of a rotor system during acceleration. In this analytical sense, if the acceleration is high and the damping is low, there may be a free vibration component that appears suddenly in the vibration triggered by the imbalance. Under these conditions, the semi-steady state assumption does not apply. In addition, Zhou and Shi [2] proposed a real-time active compensation scheme for the rapid acceleration case. Their scheme is based on the least squares estimation for imbalance [19].

The first reported research on chatter stability is done by Merritt [20], who presented a method of analyzing the stability as a function of cutting depth and speed, and presented the results by so-called a Stability Lobe Diagram (SLD). In drawing a SLD, three common methods are well-known. The first uses the Nyquist approach in which the stability is analyzed with respect to chosen cutting parameters, such as the cutting depth and the speed, and the critical values for each physical parameter are identified. The second approach is based on a Time Domain Simulation (TDS) which uses a closed loop dynamical cutting model and is performed for various cutting parameters [21]. The third approach of obtaining SLD is an analytic prediction technique, developed by Tobias and Fishwick [22]. In this technique SLD is plotted the boundary between stable and unstable cuts as a function of spindle speed and chip width. These diagrams provide a means of selecting favorable combinations of spindle speed and axial depth of cut in end milling, for example, for increased Material Removal Rates (MRR). Following this work, Fourier series expansion of time varying parameters of the centrifugal total force (F_T) has been implemented in solving the differential equations of the analytical model in an iterative manner. F_T is usually assumed linear with respect to imbalance mass of the rotating disk (m_b) and dynamic displacement of vibration $(h(t))$. The centrifugal total force (F_T) is also assumed independent of the spindle speed (ω_z). However, it is well-known that the centrifugal total force is highly nonlinear with respect to all rotating parameters. The work presented in this paper follows the footsteps of Tobias and Fishwick in simulating the cutting stability using an analytic approach [22]. The centrifugal total force (F_T) direction is assumed constant, and the rotating disk is modeled by a rigid mass and linear stiffness and damper elements. The force is determined by the x direction motion as given in Eq.(4). Stability of the system is analyzed using the Nyquist criterion in performing analytic simulations.

$$h(t) = O\vec{G}(t) = e + r_d - x(t) + x(t - \tau)$$

Using equation (12), the closed loop transfer function is obtained as;

$$\frac{X}{e} = \frac{m_b \, C \, G(s)}{1 + m_b \, C \, G(s)(1 - e^{-\tau s})} \tag{25}$$

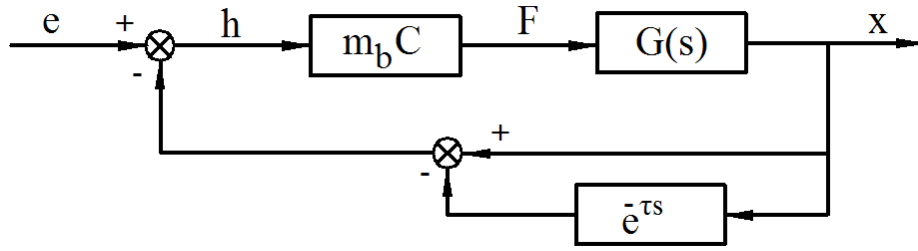The system is modeled as a closed loop controller, as shown in Figure 4,

Figure 4. Block diagram of regenerative cutting process

where $G(s)$ is the open loop transfer function obtained between the centrifugal total force (F_T) and the displacement in the $x(t)$ direction. The denominator of the closed loop transfer function is given by equation (18), and the system stability based on Nyquist criterion is determined using;

$$m_b\, C\, G(s)(1 - e^{-\tau s}) = (-1, 0\, j) \tag{26}$$

the location of the left side of Eq.(26) is studied with respect to the point (-1, 0j). This is done by first setting s=jω,

$$m_b\, C\, G(\omega)\left(1 - e^{-j\omega\tau}\right) = -1 \tag{27}$$

Next, this equation is studied in two-parts as given in Eq.(18). The left side of Eq.(18) has unit magnitude and phase of ω for all positive real frequency values, and it gives a unit circle or a critical trajectory. The right side of Eq.(18) presents a Nyquist curve, and its intersection with the unit circle determines $U_2(j\omega)$. Eq.(20) defines these frequency values. Regenerative chatter occurs at a frequency equal to the closest mode of the rotating shaft/disk system natural frequencies, and it generates a relative motion between the shaft rotating center and the disk rotating center. Thus, there is always a phase difference between two consecutive vibration wave forms, and it is given by

$$k + \frac{\varepsilon}{2\pi} = \frac{\omega_s}{n} \tag{28}$$

where k is the number of waves in one period, ε phase difference $[rad]$, ω_s rotating shaft/disk system frequency $[1/s]$; n is spindle speed $[rev/s]$. This equation corresponds to Eq.(24), where

$$\tau = \frac{2k\pi + \varepsilon}{2\pi\omega_s} \qquad \rightarrow \qquad n = \frac{60}{\tau} \tag{29}$$

$U_1(j\omega)$ and $U_2(j\omega)$ defined in Eq.(18) are simulated in Fig. 5, where for values between larger and smaller than the obtained positive real values of ω_i, U_2 curve is simulated to show if it enters into or

exits the stability region, or the unit circle. Since two roots exist, one is shown to enter while the other exits. At each delay value τ given in Eq.(20), two positive real roots exist and at these values the unit circle is intersected. The SLD is obtained by determining the imbalance mass of the rotating disk m_b for a given range of spindle speed. The limit values of imbalance mass of the rotating disk is obtained from Eq.(26) with the help of Eq.(28) as

$$m_{b\,\lim} = \frac{-1}{C\,G\left(1 - e^{-j\varepsilon}\right)} \tag{30}$$

or, by considering only the real values,

$$m_{b\,\lim} = \frac{1}{2\,C\,\mathrm{Re}\left(G(j\omega)\right)} \tag{31}$$

The SLD obtained for the two degree of freedom model in Fig. 1 is given in Fig. 6. A Matlab program was written, in generating both Fig. 5 and Fig. 6.
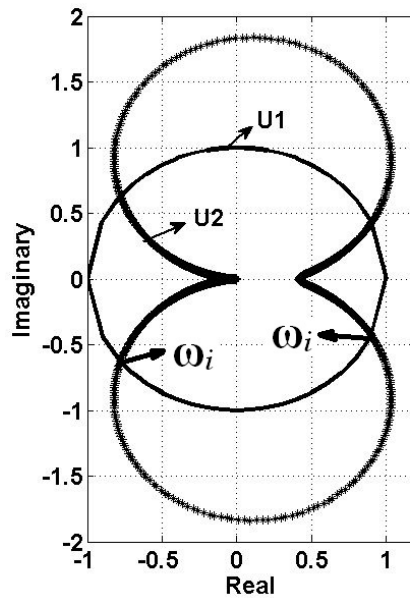

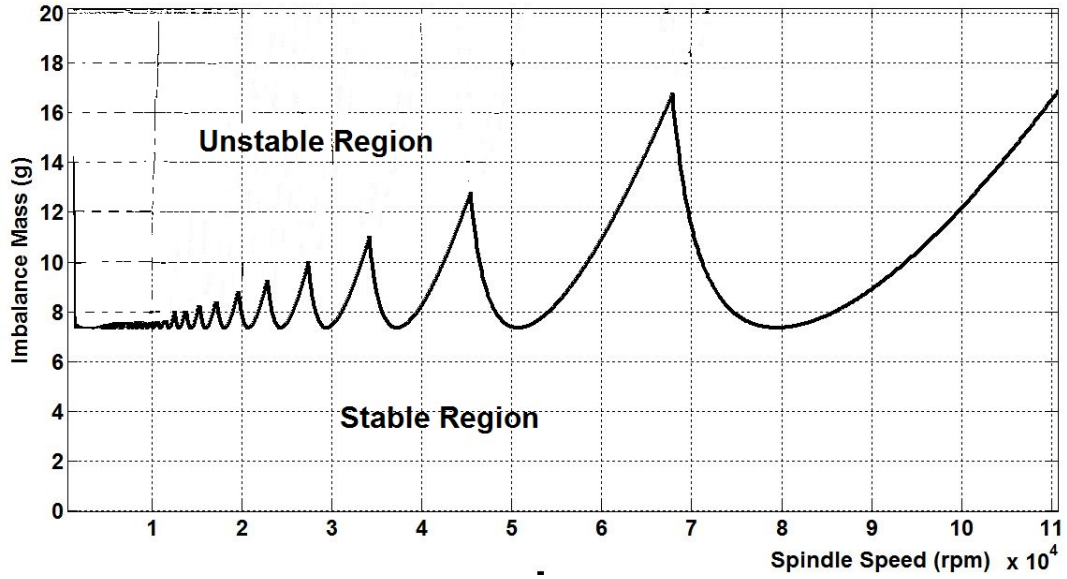**Figure 5.** Unit circle and Nyquist curve

Figure 6. Stability Lobe diagram for dynamic system.

Stability of this system was investigated by applying τ decomposition form to Nyquist criteria. The centrifugal total force, which changes in the course of time, proportionally with the dynamic reaction forces occurred from the external perpetual forces on the rotating system, is a general acceptance of linear modeling. For this reason, the constant component of the centrifugal total force F_t is neglected but variable component F_r produced by dynamic load is taken into account. According to the Nyquist criteria, the right side of this equation expresses Nyquist plane curve U_2 and the left side expresses critical orbit U_1. Thus, the positive real root of this equation gives the chatter frequency of the system as seen in Fig. 5. The above mentioned analytical method is the determination of the natural frequency of the system and mode shapes by measuring transfer functions by using an impact hammer and accelerometer. Analytical predictions of performance can be done by using this information. This analysis technique is based on the investigation of stability and plotting the SLD from the solution of the characteristic equation of the system depending on the critical parameters such as axial imbalance mass of the system and spindle speed as seen in Fig. 6. This analysis is made with the acceptance that the force process is linear according to external perpetual force and imbalance mass which doesn't depend clearly on rotating speed.

4. CONCLUSIONS

Although the model used is very simplistic and does not account for the most of the system parameters, it helps the reader get a fundamental understanding of the rotating system dynamics and stability issues. A two degree of freedom model of rotating system is developed, and the vibration phenomenon is analyzed to show how it can be prevented. The simulated results determine the critical imbalance mass of the rotating disk values as a function of the spindle speed. The results show that larger imbalance masses free of chatter can, in general, be accomplished at large speeds. However, the stability switches are unavoidable no matter how large the speed is. Large stable gaps occur at high spindle speeds, where the rotational frequency of the rotating disk is equal to the dominant natural frequency of the rotating shaft/disk structure. This stability analysis approach can be easily applied between spindle length, balancing mass amount, location of balancing mass on rotor etc. variable parameters and spindle speeds for stable rotating system. Hence, system sizing will be achieved by considering elastic modulus (E) and Yield strength (σ) of the system spindle for more stable rotating system.

REFERENCES

[1] Zhou, S., and Shi, J., Active Balancing and Vibration Control of Rotating Machinery: A Survey, The Shock and Vibration Digest, July 2001, Vol. 33, No. 4, 361-371.

[2] Zhou, S., and Shi, J., Supervisory adaptive balancing of rigid rotors during acceleration, Transactions of NAMRI/SME XXVII, 2000, 425- 430.

[3] Wowk, V., 1995, Machinery Vibration: Balancing, McGraw-Hill, New York.

[4] Gosiewski, Z., Automatic balancing of flexible rotors, part 1: theoretical background, Journal of Sound and Vibration, 1985, 100, 551-567.

[5] Gosiewski, Z., Automatic balancing of flexible rotors, part 2: synthesis of system, Journal of Sound and Vibration, 1987, 114, 103-119.

[6] Van De Vegte, J. and Lake, R. T., Balancing of rotating systems during operation, Journal of Sound and Vibration, 1978, 57, 225-235.

[7] Van De Vegte, J., Balancing of flexible rotors during operation, Journal of Mechanical Engineering Science, 1981, 23, 257-261.

[8] Knospe, C. R., Hope, R. W., Fedigan, S. J. and Williams, R. D., Experiments in the control of imbalance response using magnetic bearings, Mechanics, 1995, 5, 385-400.

[9] Knospe, C. R., Hope, R. W., Tamer, S.M. and Fedigan, S. J., Robustness of adaptive imbalance

control of rotors with magnetic bearings, Journal of Vibration and Control, 1996, 2, 33-52.

[10] Herzog, R., Buhler, P., Gahler, C. and Larsonneur, R., Imbalance compensation using generalized notch filters in the multivariable feedback of magnetic bearings, IEEE Transactions on Control Systems Technology, 1996, 4,580-586.

[11] Lum, K. Y., Coppola, V. T. and Bernstein, D. S., Adaptive autocentering control for an active magnetic bearing supporting a rotor with unknown mass imbalance, IEEE Transactions on Control Systems Technology, 1996, 4, 587-597.

[12] Li, C-J., Ulsoy, A.G. and Endres, W.J., The effect of flexible-tool rotation on regenerative ınstability in machining, Journal of Manufacturing Science and Engineering, 2003, 125, 39-47.

[13] Turkes, E., Orak, S., Neseli, S., Yaldiz, S., Linear analysis of chatter vibration and stability for orthogonal cutting in turning, Int. Journal of Refractory Metals and Hard Materials, 2011, 29, 163–169.

[14] Reinig, K. D., and Desrochers, A. A., Disturbance Accommodating Controllers for Rotating Mechanical Systems, ASME J. Dyn. Syst., Meas.,Control, 1986, 108, Mar., 24–31.

[15] Zhu, W., Castelazo, I., and Nelson, H. D., An Active Optimal Control Strategy of Rotor Vibrations Using External Forces, ASME Design Technical Conference-12th Biennial Conference on Mechanical Vibration and Noise Montreal, 1989, Que, Can 19890917-19890921.

[16] Luenberger, D. G., Observers for multivariable systems, IEEE Trans. Autom. Control, 1966, AC-11, Apr., 190–197.

[17] Knospe, C. R., Tamer, S. M., and Fittro, R., Rotor Synchronous Response Control: Approaches for Addressing Speed Dependence, J. Vib. Control, 1997, **3**, No. 4, 435–458.

[18] Zhou, S., and Shi, J., The analytical unbalance response of jeffcott rotor during acceleration, ASME J. Manuf. Sci. Eng., 2001, 123, No. 2, 99–302.

[19] Zhou, S., and Shi, J., Imbalance estimation for speed-varying rigid rotors using time-varying observer, Journal of Dynamic Systems, Measurement, and Control, 2001, 123, 637-644.

[20] Merritt, H. E., Theory of self-excited machine-tool chatter, ASME J. Eng. Ind., 1965, 87, 447–454.

[21] Landers, R.G., Ulsoy, A.G., Chatter analysis of machining systems with nonlinear force processes, ASME International Mechanical Engineering Congress and Exposition, 1996, Atlanta, Georgia, November 17-22, DSC Vol. 58, 183-190.

[22] Tobias, S., Fishwick, W., Theory of regenerative machine tool chatter, The Engineer, February, (1958).